



ELSEVIER

Available online at www.sciencedirect.com

SCIENCE @ DIRECT®

Optics Communications 235 (2004) 387–393

OPTICS
COMMUNICATIONS

www.elsevier.com/locate/optcom

Mode formation in broad area quantum dot lasers at 1060 nm

Y. Tanguy ^a, J. Muszalski ^b, J. Houlihan ^{a,*}, G. Huyet ^a, E.J. Pearce ^c,
P.M. Smowton ^c, M. Hopkinson ^d

^a *Physics Department, National University of Ireland, Cork, Ireland*

^b *Institute of Electron Technology, Al. Lotnikow 32/46, 02-668 Warsaw, Poland*

^c *Department of Physics and Astronomy, Cardiff University, Cardiff CF24 3YB, UK*

^d *EPSRC Central Facility for III-V Semiconductors, University of Sheffield, Sheffield S1 3JD, UK*

Received 12 January 2004; received in revised form 18 February 2004; accepted 18 February 2004

Abstract

An analysis of the transverse and longitudinal mode structure of broad area quantum dot lasers emitting at 1060 nm is presented. In particular, temperature is shown to play an important role in the stabilisation of the transverse mode structure of the devices. In addition, the investigation of the interaction between these transverse modes, through the measurement of the spatial intensity correlation, shows that the laser retains some modal properties in the unstable regime. Finally, measurements of spectral correlations between longitudinal mode groups display a strong dependency on their respective transverse mode structures indicating the importance of spatial overlap.

© 2004 Published by Elsevier B.V.

PACS: 42.55.Px; 42.60.Mi; 42.70.Hj

Keywords: Transverse mode; Broad-area lasers; Spatio-temporal instabilities; Quantum dots; Semiconductor lasers

1. Introduction

Quantum dot based semiconductor devices are currently being investigated by many researchers to study advantages that they may deliver over their existing quantum well counterparts. Operational insensitivity to temperature [1], low threshold currents [2], insensitivity to optical feedback [3]

and extension of existing GaAs technology into the telecommunications band are major advances which have been achieved to a certain degree. However, other aspects of devices operation such as the modulation bandwidth have not demonstrated yet such improvements although there have been some successes in addressing these shortcomings [4]. In addition to applications as replacement for a host of existing telecommunications devices, quantum dot technology has also great potential in the fields of quantum optics and quantum information as single photon sources [5,6] and single electron transistors [7].

* Corresponding author. Tel.: +353214902053; fax: +353214276949.

E-mail address: houlihan@phys.ucc.ie (J. Houlihan).

To date, much work exists on the various aspects of quantum dot laser operation. Experimental results have been published which describe filament free operation [8] and filament reduction [9] while theoretical works have shown that, even in the ideal, zero phase–amplitude coupling case, filamentation can occur [10]. Indeed, measurements of the line-width enhancement factor (alpha-factor) to date suggest that while its value can be as low as 0.1 [12], it depends strongly on the epitaxy and operating conditions, as is the case with quantum well lasers (for a recent theoretical treatment see [11]). Also, studies of the intensity noise of these devices have demonstrated that a strong anti-correlation between laser modes exists indicating a strong interaction in contention with the usual picture of a purely inhomogeneously broadened device [13]. In addition, it has been suggested that it is the homogeneous broadening that determines the often observed spectral modulation and narrowing [14], although other explanations have been put forward for spectral modulation. In fact, the broad flat gain spectrum observed for quantum dot lasers may leave the device susceptible to a range of modulating mechanisms [15]. Leaky-waveguide substrate modes [16] and transverse cavity resonances [17] have been shown to be important in certain device designs.

In this paper, we will present experimental results on mode formation in quantum dot lasers lasing at 1060 nm. We will demonstrate the importance of thermal effects and show how both the homogeneous broadening and transverse mode

structure lead to interesting features in longitudinal mode coupling phenomena.

2. Device structure

The active region of quantum dot laser structure consists of seven layers of $\text{In}_{0.5}\text{Ga}_{0.5}\text{As}$ dots within 10 nm of GaAs separated by 7 nm of $\text{Al}_{0.15}\text{Ga}_{0.85}\text{As}$. A dot density of $5 \times 10^{10} \text{ cm}^{-3}$ and base dimension of 20–25 nm are estimated [18]. Standard oxide confined devices of stripe width 50 μm and length 800 μm were fabricated and individually mounted on open heat sinks. Throughout this paper, the direction parallel to the junction will be termed transverse while the growth direction is termed lateral.

3. Mode formation and instabilities

The lasers were first analysed in a temperature stabilised, continuous wave (CW) regime (DC current supply with temperature controller ILX LDC-3714b). The total light–current (LI) characteristic and the corresponding optical spectrum of a typical device are shown on Fig. 1. The optical spectrum both below and above threshold consists of many longitudinal modes, modulated by an envelope which separates these modes into, typically, two or three different groups, depending on the laser. The power for each group of modes as a function of injection current is presented in Fig. 2. A strong competition between the two groups is

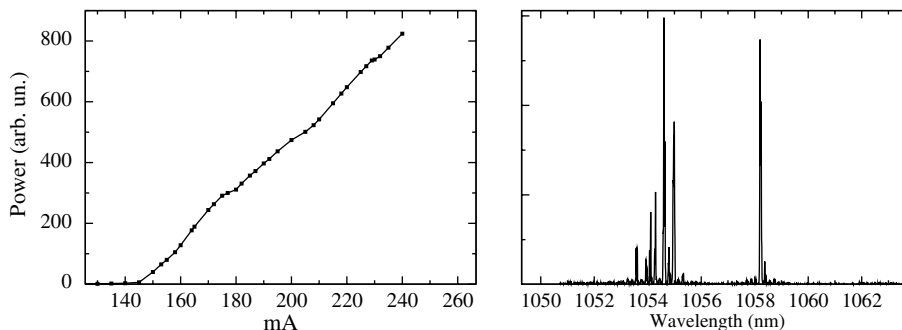


Fig. 1. Total LI curve in CW regime (left), and its spectrum at 170 mA (right).

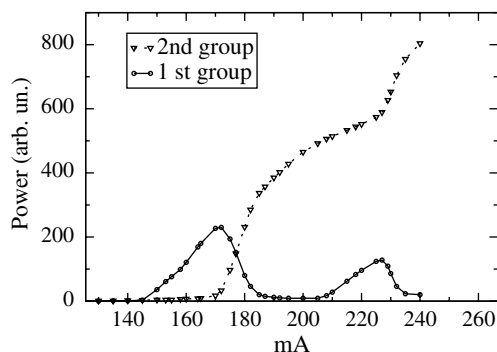


Fig. 2. Power current characteristics of each of the two spectral groups seen on Fig. 1.

apparent as the power in one group increases while the other decreases, also leading to some non-linearities in the total LI curve (Fig. 1). Similar non-linearities were also reported in [19].

The spectral components of the laser emission were separated using a two meter long monochromator as described on Fig. 3. Using this method, the transverse near field can be decomposed into its spectral components, termed the “spectrally resolved near field” (SRNF) [20]. With this technique, single transverse mode operation can be identified as a multi-lobed pattern at a precise wavelength corresponding to a particular longitudinal mode. This technique also allows the observation of a spatially varying refractive index.

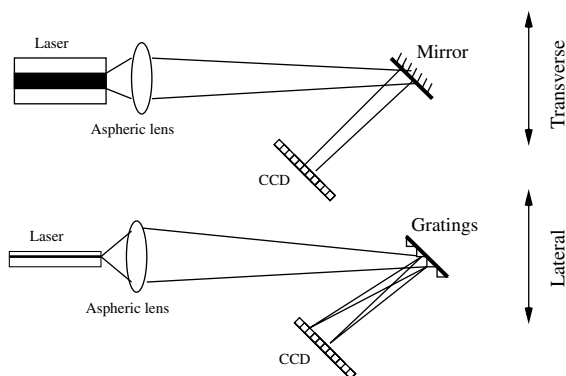


Fig. 3. Schematic of the SRNF experiment. In the lateral direction the optical field is separated into its spectral components, in the transverse direction the facet field is re-imaged on to the CCD camera.

For example, strong phase curvatures across the device, due to carrier induced anti-guiding or thermal guiding can be observed in the SRNF. In the situation where clear transverse modes are not observable in the SRNF optical filamentation can be identified by directly analysing the dynamical properties of the beam. This is necessary because the dynamical nature of filamentary operation leads to a homogeneous near field profile in average. Thus, the power of either mode group or the total was coupled to a fast-photo-detector (Newport D-30 FC, rise-time 30 ps) and examined on a high bandwidth, real time oscilloscope (LeCroy WM8000, bandwidth 6 GHz). Filamentation can be identified with a high level of broadband relaxation oscillation intensity noise.

Some SRNF's typical of low current CW operation are shown on Fig. 4. In these pictures, the formation of stable transverse modes is clearly seen. At threshold, the laser operated in the fundamental (single lobed) transverse mode. As current is increased, the mode is replaced, in turn, by the first to the fifth order mode. Within each mode group, the same transverse mode profile on each longitudinal mode was observed. However, the two groups of modes did not necessarily display the same transverse mode structure. As the injection is increased, the regular transverse mode structures and sharp longitudinal modes in the SRNF gradually disappeared in a current range of ≈ 20 mA as shown on Fig. 5. In addition, the presented time traces and corresponding intensity noise spectra demonstrate qualitatively different modes of operation. At the lower current level, the mode group displays noise below 500 MHz which may be related to various mode competition processes as well as a narrow relaxation oscillation resonance near 2 GHz. However, on increasing the current to 415 mA, the level of noise increases dramatically as can be seen on the time trace and its intensity spectrum. In addition, there is a dramatic broadening around the relaxation oscillation frequency. These features indicate that the laser is in a filamentary mode of operation. It is interesting to note that the blurring of the SRNF in both of these regimes suggests strong fluctuations of the refractive index. These fluctuations may be induced by either

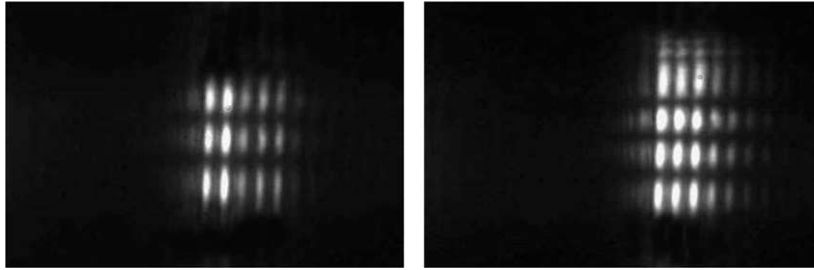


Fig. 4. SRNF in CW regime at 185 (left) and 230 mA (right) where wavelength is plotted on the abscissa and distance on the ordinate. The second and third order modes are clearly displayed.

carrier or thermal fluctuations and will be discussed in the following sections.

The carrier effects can be isolated by testing the device in pulsed mode with a low duty cycle. For these devices, pulse widths of 200 ns, delivered by a Avtech AV-107C-C with a duty cycle of 0.1%, was sufficient to ensure non-thermal operation. Generally, the clear formation of Hermite–Gaussian

transverse modes on the SRNF was *not* observed, as in the CW case. The threshold level for unstable output is much lower in the pulsed than in the CW regime. Typically, devices exhibited an unstable output at around 250–300 mA in the pulsed regime and at 360–400 mA in the CW regime. This demonstrates that the unstable regime is induced by carrier fluctuations rather than thermal processes.

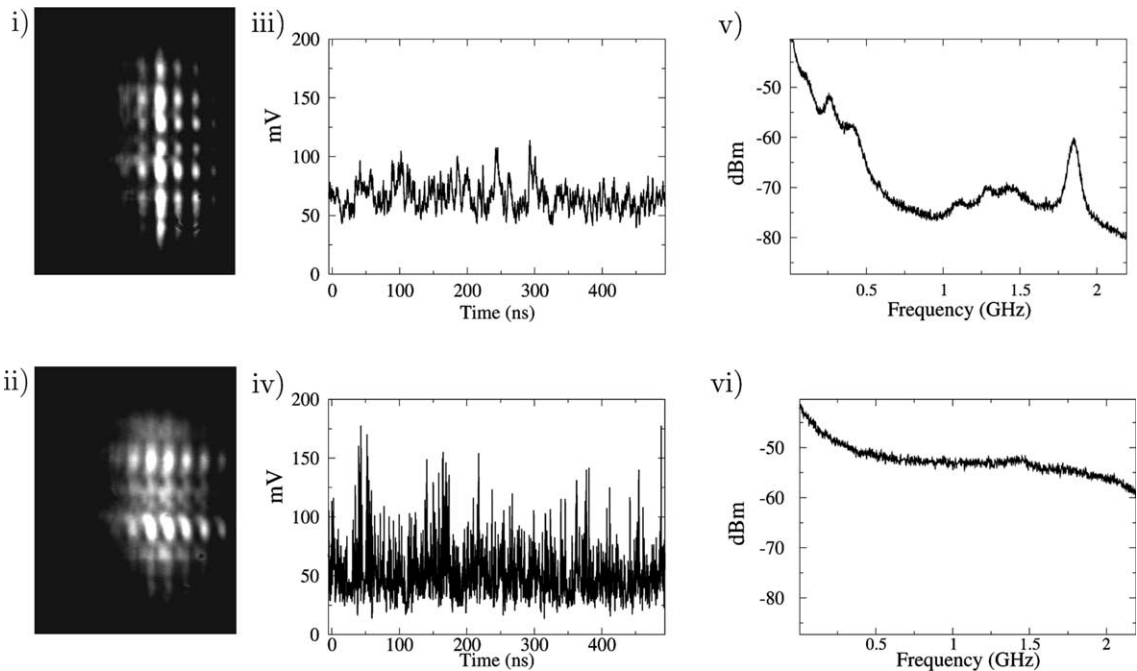


Fig. 5. SRNF in CW at 397 (i) and 415 (ii) mA where wavelength is plotted on the abscissa and distance on the ordinate. Substantial blurring has developed in both cases. Corresponding time traces at lower (iii) and higher (iv) currents. Note the increased noise at the higher current. Additionally, intensity noise spectra (v) and (vi) indicate that the instabilities at the lower current originate from mode competition phenomena. However, the increase and dramatic broadening of the noise spectrum around the relaxation oscillation frequency indicates filamentary operation.

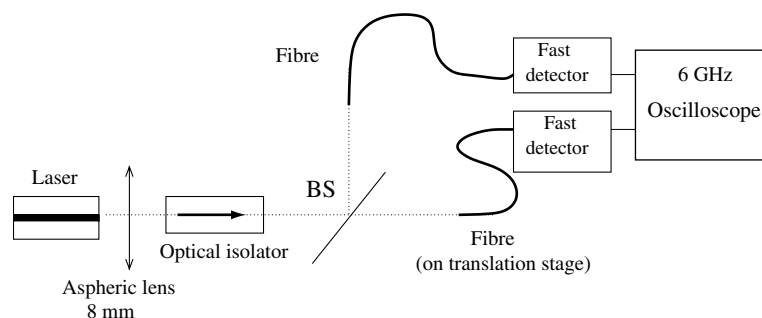


Fig. 6. Experimental apparatus to measure the correlation across the near field. One fiber is fixed when the other is moved to scan across the re-imaged near field (BS is a beam splitter).

Thermal lensing effects stabilise higher order transverse modes and modify the threshold level for unstable output. However, the carrier fluctuations can only induce a blurring of the SRNF if there are strong carrier induced refractive index fluctuations.

To further analyse this point, we measured the phase amplitude coupling in these devices just below threshold. The carrier induced refractive index shift and differential gain were both measured in the pulsed regime. Particular attention was given to ensure complete removal of all thermal effects. In order to achieve this, the shift in the longitudinal cavity spectral resonances was measured for a variety of pulse widths and duty cycles. From these measurements, the differential gain and refractive index were measured using a Hakki–Paoli scheme [21] and a variable stripe length method [22]. The alpha-factor, which is commonly used to quantify the variation of the refractive index with the differential gain [12], was calculated; we obtained a value of 4.1 ± 0.4 . This value is extremely high for a quantum dot laser but is consistent with the appearance of unstable behaviour at high output powers.

To further investigate the characteristics of the laser in the unstable regime, we measured the cross correlation between different points in the near field as shown on Fig. 6. Fig. 7 displays the result plotted with the corresponding normalised near field. The maximum of this function is one when the reference section is correlated with itself. The absolute value of the correlation decreases to either side of the reference section over a certain

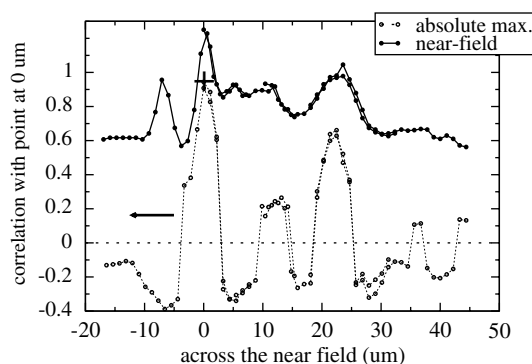


Fig. 7. Cross correlation along the re-imaged near-field when the laser is in the unstable regime (420 mA). For each point the absolute maximum of the correlation is taken. The near-field is displayed with an offset for clarity. See text for discussion.

distance before recovering somewhat. This recovery indicates that the output, while very unstable, may not be classified simply as filamentary [23] but retains some modal characteristics.

4. Relaxation oscillations and coupling

It was seen, in the previous section, that each group of longitudinal modes displays the same transverse mode and that this mode may vary from group to group. This suggests a strong coupling between longitudinal modes within each group with less coupling between groups. To measure the correlation between the groups as a function of the pump within a certain frequency bandwidth, we compute the normalised correlation coefficient [13]

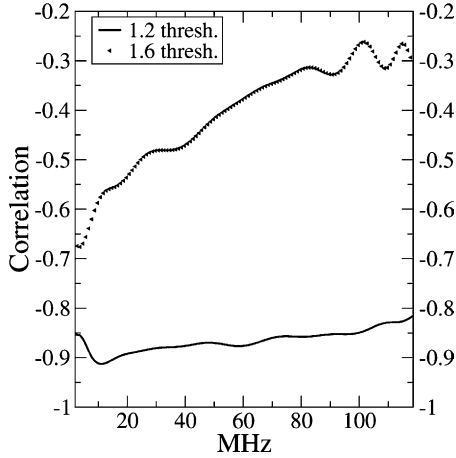


Fig. 8. Normalised correlation coefficient between the two mode groups versus the frequency, at 1.2 (lower curve) and 1.6 times threshold (upper curve).

$$C_{ij} = -\frac{S_{ij} - S_i - S_j}{2\sqrt{S_i S_j}}, \quad (1)$$

where S_i, S_j are the spectral noise powers of groups i, j and S_{ij} is the power when both groups i and j are incident on the detector at the same time. We can illustrate the behaviour of the quantity in the case of two modes with equal power, S . For perfect anti-correlation, $S_i = S_j = S$, $S_{ij} = 0$ and so $C_{ij} = -1$. Similarly, for perfect correlation, $S_i = S_j = S$, $S_{ij} = 4S$ and then $C_{ij} = 1$. Finally, if there is no correlation between the modes then $S_i = S_j = S$, $S_{ij} = 2S$ and so $C_{ij} = 0$. For our devices, the correlation at 10 MHz (1 MHz bandwidth) varied between -0.92 at $1.2I_{th}$ to -0.58 at $1.6I_{th}$. In addition the absolute value of the correlation decreased continuously with increasing frequency at $1.6I_{th}$ (see Fig. 8). These values of the correlation are quite high, indicating a strong anti-correlation between the mode groups and suggesting a strong interaction between quantum dots at different energies. Similarly high values have been reported and discussed in [13].

Next, the noise spectra around the relaxation oscillation frequency of each mode group was examined. In the lower current range of Fig. 2 (0–200 mA) both groups share a common relaxation frequency and its value depends linearly on the sum of the powers in both groups squared. This indi-

cates that the groups are strongly coupled. The coupling mechanism remains unclear but possibilities include homogeneous broadening [14] and carrier escape and recapture between different sets of quantum dots [24]. In the higher current range however, each group exhibits different relaxation oscillation frequencies which are correlated only to the squared power in each's own group. This decoupling of the relaxation oscillations occurs in the same current range as the reduction in the low frequency correlation and may be explained if we examine the corresponding SRNFs. In the low current range both groups exhibit a first order mode, indicating a high spatial overlap between groups. However, in the high current range one group switched to the second order mode, and thus the overlap has reduced. Since the homogeneous broadening, carrier escape and recapture rates should not depend on the bias level, this reduction in mode overlap is the most probable explanation for these decoupling effects. We note that spectrally resolved measurements of relaxation oscillations were also reported in [25], but without the decoupling effect, which was depicted theoretically in [26].

5. Conclusions

To summarise, in this paper we have presented experimental results which investigate mode formation in broad area quantum dot lasers at 1060 nm. These lasers have exhibited stable transverse mode operation in both pulsed and CW regime for low output powers and unstable operation for high output powers. This transition to unstable operation is delayed to higher currents in the CW regime suggesting that thermal effects may have an important role to play in future, high brightness designs. The optical spectrum of such devices tends to separate into groups of longitudinal modes, the modes within each group having an identical transverse structure indicating a strong coupling between adjacent longitudinal modes. In addition, the coupling between mode groups, while high for some parameter ranges depends strongly on the degree of spatial overlap of mode groups. We acknowledge Science Foundation Ireland for

financial support under the program SFI/01/F.1/CO13, and R. Gillen, J. Lucey and C. Roche for technical assistance.

References

- [1] Y. Arakawa, H. Sakaki, *Appl. Phys. Lett.* 40 (1982) 939.
- [2] N.N. Ledentsov et al., *Appl. Phys. Lett.* 70 (1997) 2888.
- [3] D. O'Brien et al., *Electron. Lett.* 39 (2003) 1819.
- [4] P. Bhattacharya, S. Ghosh, *Appl. Phys. Lett.* 80 (2002) 3482.
- [5] O. Benson, C. Santori, M. Pelton, Y. Yamamoto, *Phys. Rev. Lett.* 84 (2000) 2513.
- [6] C. Santori et al., *Phys. Rev. Lett.* 86 (2001) 1502.
- [7] Lei Zhuang, Lingjie Guo, Stephen Y. Chou, *Appl. Phys. Lett.* 72 (1998) 1205.
- [8] Ch. Ribbat et al., *Appl. Phys. Lett.* 82 (2003) 952.
- [9] P.M. Smowton, E.J. Pearce, H.C. Schneider, W.W. Chow, M. Hopkinson, *Appl. Phys. Lett.* 81 (2002) 3251.
- [10] C. Sailliot, V. Voignier, G. Huyet, *Opt. Commun.* 212 (2002) 353.
- [11] A.V. Uskov et al., *Appl. Phys. Lett.* 84 (2004) 272.
- [12] T.C. Newell, D.J. Bossert, A. Stintz, B. Fuchs, K.J. Malloy, L.F. Lester, *IEEE Photon. Tech. Lett.* 11 (1999) 1527.
- [13] F. Wolff et al., *Appl. Phys. Lett.* 78 (2001) 3577.
- [14] M. Sugawara, K. Mukai, Y. Nakata, H. Ishikawa, A. Sakamoto, *Phys. Rev. B* 61 (2000) 7595.
- [15] P.M. Smowton et al., *Appl. Phys. Lett.* 75 (1999) 2169.
- [16] E.P. O'Reilly, A.I. Onishenko, E.A. Avrutin, D. Bhattacharyya, J.H. Marsh, *Electron. Lett.* 34 (1998) 2035.
- [17] D. Ouyang et al., *Appl. Phys. Lett.* 81 (2002) 1546.
- [18] E. Herrmann et al., *IEE Proc. Opt.* 148 (2001) 238.
- [19] H. Horie, N. Arai, Y. Yamamoto, S. Nagao, *IEEE J. Quantum Electron.* 36 (2000) 1454.
- [20] C. Chang-Hasnain, E. Kapon, R. Bhat, *Appl. Phys. Lett.* 54 (1989) 205.
- [21] B.W. Hakki, T.L. Paoli, *J. Appl. Phys.* 46 (1975) 1299.
- [22] A. Oster, G. Erbert, H. Wenzel, *Electron. Lett.* 33 (1997) 864.
- [23] V. Voignier, J. Houlihan, J.R. O'Callaghan, C. Sailliot, G. Huyet, *Phys. Rev. A* 65 (2002) 53807.
- [24] A. Polimeni, A. Patane, M. Henini, L. Eaves, P.C. Main, *Phys. Rev. B* 59 (1999) 5064.
- [25] M. Kuntz et al., *Appl. Phys. Lett.* 81 (2002) 3846.
- [26] M. Grundmann, *Appl. Phys. Lett.* 77 (2000) 1428.